Vacancy-oxygen complexes and their optical properties in AlN epitaxial films studied by positron annihilation

A. Uedono,[1,a] S. Ishibashi,[2] S. Keller,[3] C. Moe,[3] P. Cantu,[3] T. M. Katona,[3] D. S. Kamber,[3] Y. Wu,[3] E. Letts,[3] S. A. Newman,[3] S. Nakamura,[3,4] J. S. Speck,[3,4] U. K. Mishra,[3] S. P. DenBaars,[3,4] T. Onuma,[1,4,5] and S. F. Chichibu[1,4,5]

[1]*Institute of Applied Physics, University of Tsukuba, Tsukuba, Ibaraki 305-8573, Japan*
[2]*Research Institute for Computational Sciences, National Institute of Advanced Industrial Science and Technology, Tsukuba, Ibaraki 305-8568, Japan*
[3]*Department of ECE and Department of Materials, University of California, Santa Barbara, California 93106, USA*
[4]*Nakamura Inhomogeneous Crystal Project, ERATO, Japan Science and Technology Agency, Kawaguchi 332-0012, Japan*
[5]*Center for Advanced Nitride Technology (CANTech), Institute of Multidisciplinary Research for Advanced Materials (IMRAM), Tohoku University, Sendai 980-8577, Japan*

(Received 12 November 2008; accepted 2 January 2009; published online 3 March 2009)

Vacancy-type defects in AlN grown by metal-organic vapor phase epitaxy (MOVPE) and lateral epitaxial overgrowth (LEO) using halide vapor phase epitaxy were probed by a monoenergetic positron beam. Doppler broadening spectra of the annihilation radiation were measured and compared to the spectra calculated using the projector augmented-wave method. For MOVPE-AlN, the concentration of vacancy-type defects was high near the interface between AlN and the GaN buffer layer, and the defect-rich region expanded from the interface toward the surface when the NH_3 flow rate increased. For the sample grown on the AlN buffer layer, however, the introduction of such defects was suppressed. For LEO-AlN, distinct deep emission peaks at 3–6 eV were observed in cathodoluminescence spectra. From a comparison between Doppler broadening spectra measured for LEO-AlN and computer simulated ones, an origin of the peaks was identified as complexes of Al vacancy (V_{Al}) and oxygen atoms substituting nitrogen sites such as $V_{Al}(O_N)_n$ ($n=3$ and 4). © *2009 American Institute of Physics*. [DOI: 10.1063/1.3079333]

I. INTRODUCTION

Aluminum nitride (AlN) has a large direct band gap (Ref. 1: 6.04 eV) and exhibits unique properties such as high mechanical hardness, high thermal conductivity, low thermal expansion, a large dielectric constant, and high resistance to chemicals and radiation. AlN and its alloy AlGaN are therefore potential materials for high-power electronic and optical devices which can be used in the blue to ultraviolet wavelength region.[1] Deep-ultraviolet light-emitting diodes (LED) based on AlGaN have been intensively investigated,[2,3] and an AlN-based LED with a wavelength of 210 nm has been demonstrated.[4] Generally, however, such optical devices have exhibited low external quantum efficiency, which can be associated with high-density nonradiative recombination centers (NRCs) present in AlGaN.[5] The reduction of threading dislocations that mainly originate from the lattice mismatch between substrates and films is crucial because they are thought to act as one of the major NRCs in blue-laser diodes.[6,7] Native point defects and their complexes with impurities are also expected to influence the optical and electrical properties of AlN-based devices.[8–11] Oxygen is the major residual impurity in AlN. Oxygen atoms substitute nitrogen sites and form complexes with Al vacancies (V_{Al}) (Ref. 12) which have been associated with a characteristic deep emission band in the energy range between 3 and 5 eV.[13–16] Although native point defects are known to affect the properties of AlN, information about their nature is limited at this stage.

Positron annihilation is a powerful technique for evaluating vacancy-type defects in semiconductors.[17] Point defects in AlGaN have been investigated using this method,[5,18–21] and the results show that positrons are a useful probe for studying point defects in AlN and its alloys. In the present study, we have used a monoenergetic positron beam to probe vacancy-type defects in AlN grown by metal-organic vapor phase epitaxy (MOVPE) and lateral epitaxial overgrowth (LEO) using halide vapor phase epitaxy (HVPE).

When a positron is implanted into condensed matter, it annihilates with an electron and emits two 511 keV γ quanta.[17] The energy distribution of the annihilation γ rays is broadened by the momentum component of the annihilating electron-positron pair, p_L, which is parallel to the direction of the γ rays. The energy of the γ rays is given by $E_\gamma = 511 \pm \Delta E_\gamma$ keV. Here, the Doppler shift, ΔE_γ, is given by $\Delta E_\gamma = p_L c/2$, where c is the speed of light. A freely diffusing positron may be localized in a vacancy-type defect due to Coulomb repulsion from ion cores. Because the momentum distribution of the electrons in such defects differs from that of electrons in the bulk material, these defects can be detected by measuring the Doppler broadening spectra of the annihilation radiation. The resultant changes in the spectra are characterized by the S parameter, which mainly reflects changes due to the annihilation of positron-electron pairs

[a]Electronic mail: uedono@sakura.cc.tsukuba.ac.jp

with a low-momentum distribution, and by the *W* parameter, which mainly characterizes changes due to the annihilation of pairs with a high-momentum distribution. In general, the characteristic value of *S* (*W*) for the annihilation of positrons trapped by vacancy-type defects is larger (smaller) than that for positrons annihilated from the free state.

II. EXPERIMENT

The samples investigated were AlN epitaxial films grown on a *c*-plane sapphire substrate by MOVPE and an AlN film grown on the patterned SiC substrate by LEO using HVPE. Growth conditions similar to those used for the present samples and the sample properties have been reported elsewhere.[22,23] For MOVPE-AlN,[22] before the deposition of AlN films, a 14-nm-thick GaN or a 9-nm-thick AlN buffer layer was deposited on the substrates at 630 and 1000 °C, respectively. AlN films with a thickness of 730 nm were grown on the GaN/sapphire template. The sources of Al and nitrogen were trimethylaluminum (TMAl) and NH_3, where the flow rate of TMAl was fixed at 40 SCCM (SCCM denotes cubic centimeter per minute at STP) and the NH_3 flow rates were 5 and 30 SCCM. A 650-nm-thick AlN film was deposited on the AlN/sapphire template, where the TMAl and NH_3 flow rates were 40 and 18 SCCM, respectively. For all samples, the deposition temperature was 1260 °C. Using secondary ion mass spectroscopy, the major impurity in the AlN films was found to be oxygen and its concentration was $10^{19}-10^{20}$ cm^{-3}.

For LEO-AlN,[23] a 22-μm-thick AlN film was grown on the patterned 6H-SiC substrate. Prior to the growth of the AlN film, standard photolithography was used to prepare approximately 5-μm-wide stripes separated by 5-μm-wide openings. The AlN film was grown on the substrate using a two-zone horizontal directed-flow HVPE system. The film was grown at atmospheric pressure with the substrate temperature in excess of 1200 °C. The cathodoluminescence (CL) of the sample was measured at 11 K, where the current density and the acceleration energy were 1.5×10^{-2} A/cm^2 and 3.5 keV, respectively. Details of the measurement system are described elsewhere.[20] The oxygen concentration was about 10^{19} cm^{-3}.

With a monoenergetic positron beam, the Doppler broadening spectra of the annihilation radiation were measured with a Ge detector as a function of the incident positron energy *E*. For each incident positron energy *E*, a spectrum with about 1×10^6 counts was obtained. The low-momentum part was characterized by the *S* parameter, defined as the number of annihilation events over the energy range of 511 keV $\pm\Delta E_\gamma$ (where ΔE_γ=0.76 keV) around the center of the peak. The relationship between *S* and *E* was analyzed by VEPFIT, a computer program developed by van Veen *et al.*[24] The *S*-*E* curve was fitted using

$$S(E)=S_sF_s(E)+\Sigma S_iF_i(E), \tag{1}$$

where $F_s(E)$ is the fraction of positrons annihilated at the surface and $F_i(E)$ is the fraction annihilated in the *i*th layer $[F_s(E)+\Sigma F_i(E)=1]$. S_s and S_i are *S* parameters corresponding, respectively, to the annihilation of positrons on the surface and in the *i*th layer. To examine the annihilation characteristics of positrons in detail, we used a coincidence-detection system.[15] Spectra with about 5×10^6 counts were obtained and then characterized using the *S* and *W* parameter (the *W* value was calculated from the tail of the peak, in the range of 3.4 keV $\leq|\Delta E_\gamma|\leq$ 6.8 keV).

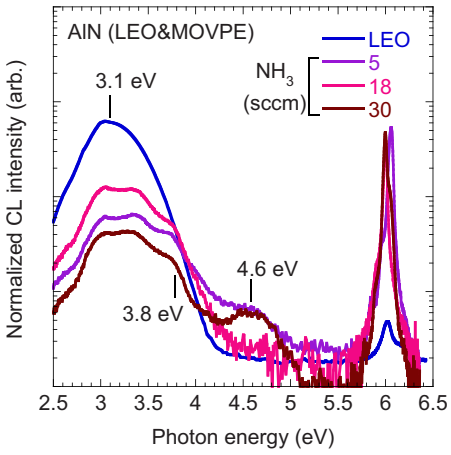

FIG. 1. (Color online) Normalized CL spectra measured at 11 K for LEO-AlN and MOVPE-AlN grown with NH_3 flow rates of 5, 18, and 30 SCCM. The spectra exhibited NBE excitonic emission peaks around 6 eV and the deep emission bands at 3.1, 3.8, and 4.6 eV.

Doppler broadening spectra corresponding to the annihilation of positrons in vacancy-type defects were theoretically calculated from valence-electron wave functions obtained by the projector augmented-wave (PAW) method[25–27] using our in-house QMAS (Quantum MAterials Simulator) code.[28] In this method, since the wave functions exhibit correct behavior near ion cores, the corresponding electron-positron momentum densities in a higher momentum region can be obtained with better accuracy than by using the norm-conserving pseudopotential (NCPP) method. The difference between results obtained by the PAW and NCPP methods is described elsewhere.[29] For the exchange and correlation energies for electrons, the generalized gradient approximation[30] was used together with partial core correction.[31] The plane-wave cutoff energy was set to 20 hartree. The formalism of the local density approximation[32] was used for the calculation of the positron wave functions. The structural optimization was made for a cell containing about 128 atoms by means of *ab initio* quenched molecular dynamics.

III. RESULTS AND DISCUSSION

Figure 1 shows CL spectra for LEO-AlN and MOVPE-AlN grown with NH_3 flow rates of 5, 18, and 30 SCCM. For MOVPE-AlN, the spectra were normalized to the near-band-edge (NBE) peak intensity. The NBE peak was assigned primarily to the recombination of excitons bound to a neutral donor (D^0,X), and the observed variation in the peak positions can be associated with the residual stress in the films.[18] The emission bands observed at 3–5 eV have been invoked as donor-acceptor-pair (DAP) recombinations and associated with Al vacancy (V_{Al}) related defects such as complexes between V_{Al} and oxygen atoms substitute nitrogen site (O_N).[11–14] For LEO-AlN, the observed intensity of the deep

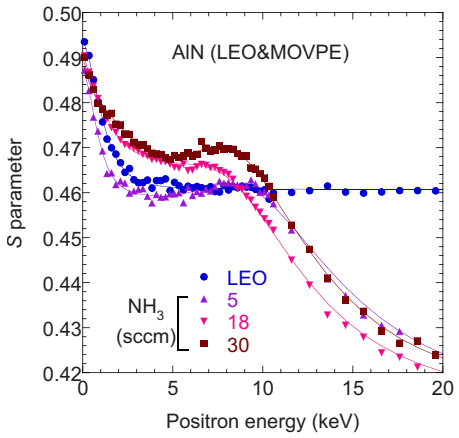

FIG. 2. (Color online) *S* parameters as a function of incident positron energy *E* for AlN grown using LEO and MOVPE with NH_3 flow rates of 5, 18, and 30 SCCM. The solid curves are fits to the experimental data. The derived depth distributions of *S* are shown in Fig. 3.

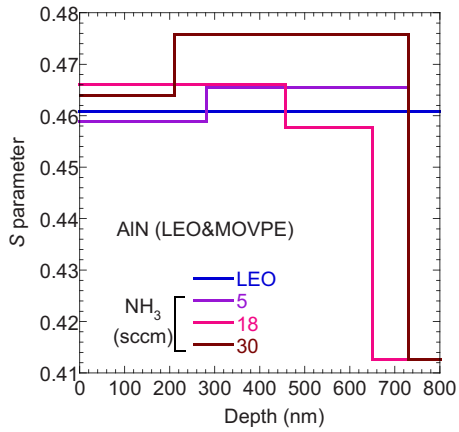

FIG. 3. (Color online) Depth distribution of *S* for AlN grown using LEO and metal-organic chemical-vapor deposition (MOCVD) obtained from the analysis of the *S*-*E* curves.

emission band was far stronger than that for MOVPE-AlN. The ratio of the integrated peaks of the NBE emission to the DAP recombination was calculated to be 690, while that for MOVPE-AlN ranged from 2 to 9. This suggests that the concentration of DAP recombination centers in LEO-AlN was higher than that in MOVPE-AlN.

Figure 2 shows the *S* values of AlN films grown using LEO and MOVPE with NH_3 flow rates of 5, 18, and 30 SCCM as a function of incident positron energy *E*. The observed increase in the *S* values at low *E* (<2 keV) is associated with the annihilation of positrons at the surface, and those above $E=4-5$ keV correspond to the annihilation of positrons in the AlN films. The decrease in the *S* value at high *E* (>10 keV) is due to the annihilation of positrons in the substrate. The observed *S*-*E* curves were fitted using Eq. (1). In the fitting procedure, a homogeneous defect distribution was assumed for LEO-AlN. For MOVPE-AlN, the region detected by positrons was divided into two blocks, and the width of the first block and the *S* value for each block were derived from the fitting. The effect of the annihilation of positrons in the buffer layers on the *S* value was neglected. The solid curves are fits to the experimental data, and the derived depth distributions of the *S* values are shown in Fig. 3.

For MOVPE-AlN fabricated using the GaN buffer layer (NH_3 flow rate=5 and 30 SCCM), the *S* value near the AlN/GaN interface was higher than that in the subsurface region. From the first-principles calculation, it was suggested that the charge state of V_N is positive[8,12] and it is expected to repel positrons by Coulomb interaction. The major species of the vacancy-type defects detected by positrons, therefore, is neutral and/or negatively charged defects such as Al vacancies (V_{Al}) and vacancy clusters. For MOVPE-AlN fabricated using the AlN buffer layer (NH_3 flow rate=18 SCCM), this was not the case. Thus, in the fabrication of AlN, since vacancy-type defects tend to be introduced from the AlN/GaN interface, a certain film thickness is required to avoid the effect of the interface. In Fig. 1, an emission peak at 4.6 eV was observed for MOVPE-AlN grown on the GaN/sapphire temperate (NH_3 flow rate=5 and 18 SCCM), but this was not the case for AlN grown on the AlN/sapphire temperate and LEO-AlN. Thus, this emission peak could relate to the defects near the interface between AlN and the GaN buffer layer.

The diffusion length of positrons (L_d) is a useful parameter for the characterization.[17,18] The relationship between L_d and the positron trapping rate (κ_d) is $L_d=\sqrt{D_+/\lambda_{\text{eff}}}$, where D_+ is the diffusion constant of positrons and λ_{eff} is the effective annihilation rate of positrons. If the positron trapping by defects is taken into account, λ_{eff} is given by $\lambda_{\text{eff}}=\lambda_f+\mu_d C_d$, where λ_f, μ_d, and C_d are the annihilation rate from the free state, the trapping coefficient, and the defect concentration, respectively ($\kappa_d=\lambda_f+\mu_d C_d$). For LEO-AlN, the value of L_d was derived from the fitting to be 12 ± 1 nm. For MOVPE-AlN with NH_3 flow rates of 5, 18, and 30 SCCM, the L_d values were determined as 8 ± 1, 20 ± 1, and 49 ± 3 nm, respectively. For MOVPE-AlN fabricated using the AlN buffer layer, for example, although the *S* value was larger than that for LEO-AlN, the L_d value was higher than that for LEO-AlN. Generally, the trapping of positrons by vacancy-type defects increases the *S* value and decreases the L_d value. One explanation for the observed incoherence is that defects exhibiting a small characteristic *S* value would be present in LEO-AlN.

The value of κ_d can be calculated as $\kappa_d=\lambda_f[(L_{d(f)}/L_d)^2-1]$, where λ_f and $L_{d(f)}$ are, respectively, the annihilation rate and the diffusion length of positrons in defect-free AlN [the positron lifetime in defect-free AlN (τ_f) is $\tau_f=1/\lambda_f$]. We can estimate the trapping fraction of positrons (F_d) as $F_d=\kappa_d/(\lambda_f+\kappa_d)$. The L_d value for defect-free AlN was not known at this stage. Uedono and co-workers[33,34] reported that positrons annihilate from the delocalized state in high-quality GaN and the diffusion length of positrons is 50–100 nm. Using those values as the defect-free diffusion length in AlN and the τ_f value reported by Slotte *et al.*[19] (157 ps), we obtained an F_d value of 0.9–1.0 for LEO-AlN. This suggests that almost all positrons annihilate in the trapped state in LEO-AlN and the obtained *S* value for the film is the characteristic value for such a state.

In the present work, we discuss the defect species of AlN from a comparison between Doppler broadening spectra ob-

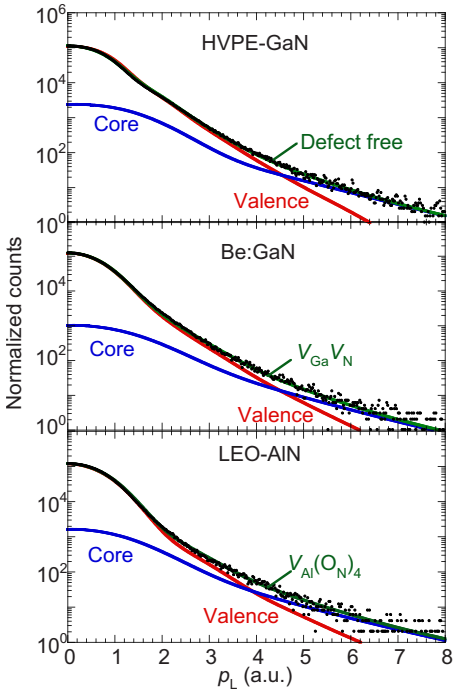

FIG. 4. (Color online) Coincidence Doppler broadening spectra (black dots) for (a) HVPE-GaN, (b) Be-implanted GaN (Ref. 32), and (c) LEO-AlN. Green curves were obtained using the PAW method for (a) the delocalized state, (b) the trapped state by $V_{Ga}V_N$ in GaN, and (c) the trapped state by $V_{Al}(O_N)_4$ in AlN. Blue and red curves show the annihilation of positrons with core and valence electrons, respectively.

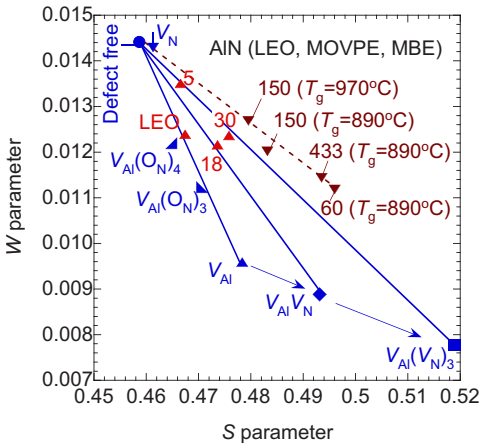

FIG. 5. (Color online) *S*-*W* relationships for AlN grown by LEO, MOCVD, and MBE. Red symbols show the results for the present experiment (LEO- and MOVPE-GaN). Brown symbols show the results for AlN grown by NH_3-source MBE (Ref. 18) where the V/III ratio (60, 150, and 433) and the growth temperatures (T_g) are shown in the figure. The (S,W) values (blue) were obtained through the PAW method for positron annihilation in the defect-free, V_{Al}, V_N, $V_{Al}V_N$, and $V_{Al}(V_N)_3$ samples. The calculation results for defect complexes between V_{Al} and oxygen atoms substituting nitrogen sites [$V_{Al}(O_N)_3$ and $V_{Al}(O_N)_4$] are also shown. Arrows (blue) show the effect of the V_N on the (S,W) value.

tained through the experiments and ones calculated using the PAW method. To show the applicability of the calculation to identify defects, prior to examining AlN, we studied the annihilation characteristics of positrons in high-quality GaN.[34,35] The spectrum for HVPE-GaN is shown in Fig. 4(a). The positron lifetime obtained for this sample was 153 ± 1 ps. Since the lifetime is close to the lifetime of positrons that annihilate from the delocalized state, the spectrum for HVPE-GaN is close to the characteristic one for defect-free GaN. In Fig. 4(a), the solid green curve was obtained using calculations for the annihilation of positrons from the delocalized state, where the blue and the red curves, respectively, show the annihilation of positrons with core and valence electrons. The spectrum corresponding to the annihilation of positrons in the damaged region in Be-implanted GaN (Ref. 34) is shown in Fig. 4(b). For ion implanted GaN, the major defect species detected by positrons was identified as Ga vacancies (V_{Ga}) and/or divacancies ($V_{Ga}V_N$).[34] The calculated spectrum for the trapping of positrons by $V_{Ga}V_N$ is shown in Fig. 4(b). In Figs. 4(a) and 4(b), the calculated spectrum agreed well with the spectrum measured experimentally.

Figure 5 shows the (S,W) values for Doppler broadening profiles obtained using the PAW method (blue symbols), where calculations were made for the annihilation of positrons from the delocalized state and the trapped states by V_{Al}, V_N, and vacancy complexes such as $V_{Al}V_N$ and $V_{Al}(V_N)_3$. The (S,W) values for the complexes between V_{Al} and oxygen atoms [$V_{Al}(O_N)_3$ and $V_{Al}(O_N)_4$] are also shown. The atomic geometries for those vacancy complexes are shown in Fig. 6.

The (S,W) value for V_N was almost identical to that for the delocalized state (defect free). This suggests that the positron annihilation is not sensitive enough for detection of isolated V_N, even if positrons annihilate in such defects. The effect of V_N, however, can be seen when it makes complexes with V_{Al}; the increase in the number of V_N results in a rightward shift in the *S*-*W* plot (blue arrows). A similar tendency of the defect complexes was obtained for GaN.[34,35]

Figure 5 shows the (S,W) values corresponding to the positron annihilation in AlN fabricated by LEO and MOVPE (red symbols). The figure also shows results for molecular beam epitaxy (MBE)-AlN fabricated with different V/III ratios (60, 150, and 433) and growth temperatures (T_g=890 and 970 °C).[20] For LEO-AlN, the observed (S,W) value was close to the calculated value for $V_{Al}(O_N)_4$. The comparison between the Doppler broadening spectra for LEO-AlN and $V_{Al}(O_N)_4$ is shown in Fig. 4(c) and reasonable agreement was obtained. In the present experiments, however, the number of defect species detected by positrons was not confirmed to be 1. In this case, the (S,W) value obtained as a weighted average of the characteristic values for the defects. In addition, since the difference between the (S,W) value for $V_{Al}(O_N)_3$ and $V_{Al}(O_N)_4$ is not large, separation of those defects is difficult. Thus, one can conclude that the major defect species detected by positrons is the complexes between V_{Al} and oxygen in LEO-AlN, and the mean number of oxygen coupled with V_{Al} is 3–4. The deep emission in AlN with high oxygen concentration has been associated with a DAP emission involving $V_{Al}^{-3} - 3 \times O_N^+$ complexes.[13–16] Because the charge states of V_{Al}-oxygen complexes are expected to depend on the Fermi level position or on the presence of other unintentionally doped impurities (such as Si), $V_{Al}(O_N)_4$ is still a DAP center candidate.

For MOVPE-AlN using the AlN buffer (NH_3 flow rate =18 SCCM), the (S,W) value was also close to the values

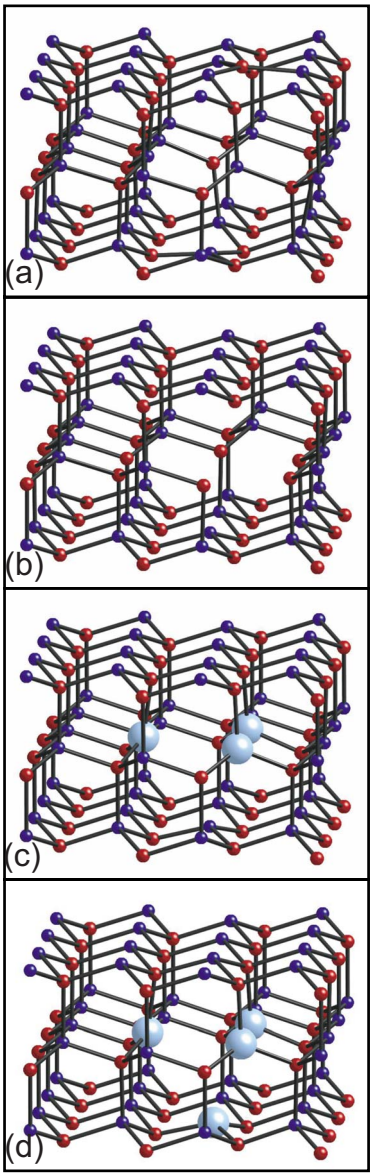

FIG. 6. (Color online) Atomic configurations obtained through the PAW method for (a) $V_{Al}V_N$, (b) $V_{Al}(V_N)_3$, (c) $V_{Al}(O_N)_3$, and (d) $V_{Al}(O_N)_4$. The red, blue, and light-blue spheres represent Al, nitrogen, and oxygen atoms, respectively.

for $V_{Al}(O_N)_3$ and $V_{Al}(O_N)_4$. Since the intensity of the deep emission band was higher than that of other MOPVE-AlN samples, the conclusion obtained for LEO-AlN was confirmed. As shown in Fig. 5, for MOVPE-AlN and MBE-AlN, the increase in the S values (or introduction of vacancy-type defects) caused a rightward shift and the value did not approach the characteristic value for isolated V_{Al}. Thus, the major defect species in such AlN films can be identified as vacancy clusters such as $V_{Al}(V_N)_n$ $(n=1-3)$. In the present experiments, the effect of the positron annihilation near the interface between AlN and the buffer layer was not negligible. Thus, the defects indentified above could be present in such regions.

IV. SUMMARY

We have used a monoenergetic positron beam to probe vacancy-type defects in AlN grown using MOVPE and LEO with HVPE. Doppler broadening spectra were measured as a function of the incident energy of positrons. The Doppler broadening spectra corresponding to the annihilation of positrons from the delocalized and localized states in vacancy-type defects were calculated using the PAW method. From a comparison between the (S,W) values obtained by the experiments and by theory, we determined the defect species detected by positrons. For MOVPE-AlN grown on the GaN/sapphire temperate, the S value corresponding to the annihilation of positrons near the interface between AlN and the buffer layer was high and the defect-rich region expanded from the interface toward the surface with an increasing NH_3 flow rate. However, no increase in the S value near the buffer layer was observed for the sample grown on the AlN/sapphire template. This suggests that defect control near the interface is a key to obtaining high-quality AlN because the interface is a source of the vacancy-type defects. For LEO-AlN, the species of the major point defects were identified as complexes between V_{Al} and oxygen such as $V_{Al}(O_N)_n$ $(n=3$ and 4), and such complexes were associated with an origin of the distinct deep emission band at 3–5 eV. A similar phenomenon was also observed for MOVPE-AlN grown on the AlN buffer layer. The observed results suggest a strong correlation between V_{Al} and oxygen atoms in AlN. In turn, if one might be able to introduce isolated V_{Al} in the restricted region, they could be used as a getter of residual oxygen in AlN. We have shown that the positron annihilation parameter is sensitive to vacancy-impurity complexes in AlN and that data analysis using the relationship between S and W with computer simulations can be a useful tool for determining defect behaviors in AlN.

ACKNOWLEDGMENTS

Part of this study was financially supported by grants in aid of Scientific Research in Priority Areas under Contract No. 18069001 "Optoelectronics Frontier by Nitride Semiconductor-Ultimate Utilization of Nitride Semiconductor Material Potential" by the Ministry of Education, Culture, Sports, Science, and Technology and of "Next Generation Super Computing Project, Nanoscience Program."

[1] S. F. Chichibu, A. Uedono, T. Onuma, B. A. Haskell, A. Chakraborty, T. Koyama, P. T. Fini, S. Keller, S. P. DenBaars, J. S. Speck, U. K. Mishra, S. Nakamura, S. Yamaguchi, S. Kamiyama, H. Amano, I. Akasaki, J. Han, and T. Sota, Nature Mater. **5**, 810 (2006).
[2] M. Asif Khan, M. Shatalov, H. P. Maruska, H. M. Wang, and E. Kuokstis, Jpn. J. Appl. Phys. **44**, 7192 (2005).
[3] For a review, see, for example, H. Hirayama, J. Appl. Phys. **97**, 091101 (2005).
[4] Y. Taniyasu, M. Kasu, and T. Makimoto, Nature (London) **441**, 325 (2006).
[5] S. F. Chichibu, A. Uedono, T. Onuma, S. P. DenBaars, U. K. Mishra, J. S. Speck, and S. Nakamura, Mater. Sci. Forum **590**, 233 (2008).
[6] S. Nakamura, M. Senoh, S. I. Nagahama, N. Iwasa, T. Yamada, T. Matsushita, H. Kiyoku, Y. Sugimoto, T. Kozaki, H. Umemoto, M. Sano, and K. Chocho, J. Cryst. Growth **189–190**, 820 (1998).
[7] M. Hansen, P. Fini, L. Zhao, A. C. Abare, L. A. Coldren, J. S. Speck, and S. P. DenBaars, Appl. Phys. Lett. **76**, 529 (2000).
[8] C. Stampfl and C. G. Van de Walle, Phys. Rev. B **65**, 155212 (2002).
[9] Q. Zhou and M. O. Manasreh, Appl. Phys. Lett. **80**, 2072 (2002).
[10] N. Nepal, K. B. Nam, M. L. Nakarmi, J. Y. Lin, H. X. Jiangm, J. M. Zavada, and R. G. Wilson, Appl. Phys. Lett. **84**, 1090 (2004).
[11] S. M. Evans, N. C. Giles, L. E. Halliburton, G. A. Slack, S. B. Schujman,

and L. J. Schowalter, Appl. Phys. Lett. **88**, 062112 (2006).
[12]T. Mattila and R. M. Nieminen, Phys. Rev. B **54**, 16676 (1996).
[13]G. A. Slack, L. J. Schowalter, D. Morellic, and J. A. Freitas, Jr., J. Cryst. Growth **246**, 287 (2002).
[14]M. Kazan, B. Ruffé, Ch. Zgheib, and P. Masri, J. Appl. Phys. **98**, 103529 (2005).
[15]E. Monroy, J. Zenneck, G. Cherkashinin, and O. Ambacher, Appl. Phys. Lett. **88**, 071906 (2006).
[16]A. Dadgar, A. Krost, J. Christen, B. Bastek, F. Bertram, A. Krtschil, T. Hempel, J. Bläsing, U. Haboeck, and A. Hoffmann, J. Cryst. Growth **297**, 306 (2006).
[17]R. Krause-Rehberg and H. S. Leipner, *Positron Annihilation in Semiconductors, Solid-State Sciences* (Springer-Verlag, Berlin, 1999), Vol. 127.
[18]T. Onuma, S. F. Chichibu, A. Uedono, T. Sota, P. Cantu, T. M. Katona, J. F. Keading, S. Keller, U. K. Mishra, S. Nakamura, and S. P. DenBaars, J. Appl. Phys. **95**, 2495 (2004).
[19]J. Slotte, F. Tuomisto, K. Saarinen, C. G. Moe, S. Keller, and S. P. DenBaars, Appl. Phys. Lett. **90**, 151908 (2007).
[20]T. Koyama, M. Sugawara, T. Hoshi, A. Uedono, J. F. Kaeding, R. Sharma, S. Nakamura, and S. F. Chichibu, Appl. Phys. Lett. **90**, 241914 (2007).
[21]F. Tuomisto, J.-M. Mäki, T. Yu. Chemekova, Yu. N. Makarov, O. V. Avdeev, E. N. Mokhov, A. S. Segal, M. G. Ramm, S. Davis, G. Huminic, H. Helava, M. Bickermann, and B. M. Epelbaum, J. Cryst. Growth **310**, 3998 (2008).
[22]H. Ikeda, T. Okamura, K. Matsukawa, T. Sota, M. Sugawara, T. Hoshi, P. Cantu, R. Sharma, J. F. Kaeding, S. Keller, U. K. Mishra, K. Kosaka, K. Asai, S. Sumiya, T. Shibata, M. Tanaka, J. S. Speck, S. P. DenBaars, S. Nakamura, T. Koyama, T. Onuma, and S. F. Chichibu, J. Appl. Phys. **102**, 123707 (2007).
[23]D. S. Kamber, Y. Wu, E. Letts, S. P. DenBaars, J. S. Speck, S. Nakamura, and S. A. Newman, Appl. Phys. Lett. **90**, 122116 (2007).
[24]A. van Veen, H. Schut, J. de Vries, R. A. Hakvoort, and M. R. Ijpma, AIP Conf. Proc. **218**, 171 (1991).
[25]P. E. Blöchl, Phys. Rev. B **50**, 17953 (1994).
[26]N. A. W. Holzwarth, G. E. Matthews, R. B. Dunning, A. R. Tackett, and Y. Zeng, Phys. Rev. B **55**, 2005 (1997).
[27]G. Kresse and D. Joubert, Phys. Rev. B **59**, 1758 (1999).
[28]S. Ishibashi, T. Tamura, S. Tanaka, M. Kohyama, and K. Terakura, (unpublished).
[29]S. Ishibashi, Mater. Sci. Forum **445–446**, 401 (2004).
[30]J. P. Perdew, K. Burke, and M. Ernzerhof, Phys. Rev. Lett. **77**, 3865 (1996).
[31]S. G. Louie, S. Froyen, and M. L. Cohen, Phys. Rev. B **26**, 1738 (1982).
[32]E. Boroński and R. M. Nieminen, Phys. Rev. B **34**, 3820 (1986).
[33]A. Uedono, S. F. Chichibu, Z. Q. Chen, M. Sumiya, R. Suzuki, T. Ohdaira, T. Mikado, T. Mukai, and S. Nakamura, J. Appl. Phys. **90**, 181 (2001).
[34]A. Uedono, K. Ito, H. Nakamori, K. Mori, Y. Nakano, T. Kachi, S. Ishibashi, T. Ohdaira, and R. Suzuki, J. Appl. Phys. **102**, 084505 (2007).
[35]A. Uedono, C. Shaoqiang, S. Jongwon, K. Ito, H. Nakamori, N. Honda, S. Tomita, K. Akimoto, H. Kudo, and S. Ishibashi, J. Appl. Phys. **103**, 104505 (2008).